ORIGINAL ARTICLE

Deregulation of MicroRNAs mediated control of carnitine cycle in prostate cancer: molecular basis and pathophysiological consequences

A Valentino[1], A Calarco[1], A Di Salle[1], M Finicelli[2], S Crispi[2], RA Calogero[3], F Riccardo[3], A Sciarra[4], A Gentilucci[4], U Galderisi[5], S Margarucci[2] and G Peluso[1]

Cancer cells reprogram their metabolism to maintain both viability and uncontrolled proliferation. Although an interplay between the genetic, epigenetic and metabolic rewiring in cancer is beginning to emerge, it remains unclear how this metabolic plasticity occurs. Here, we report that in prostate cancer cells (PCCs) microRNAs (miRNAs) greatly contribute to deregulation of mitochondrial fatty acid (FA) oxidation via carnitine system modulation. We provide evidence that the downregulation of hsa-miR-124-3p, hsa-miR-129-5p and hsa-miR-378 induced an increase in both expression and activity of CPT1A, CACT and CrAT in malignant prostate cells. Moreover, the analysis of human prostate cancer and prostate control specimens confirmed the aberrant expression of miR-124-3p, miR-129-5p and miR-378 in primary tumors. Forced expression of the miRNAs mentioned above affected tumorigenic properties, such as proliferation, migration and invasion, in PC3 and LNCaP cells regardless of their hormone sensitivity. CPT1A, CACT and CrAT overexpression allow PCCs to be more prone on FA utilization than normal prostate cells, also in the presence of high pyruvate concentration. Finally, the simultaneous increase of CPT1A, CACT and CrAT is fundamental for PCCs to sustain FA oxidation in the presence of heavy lipid load on prostate cancer mitochondria. Indeed, the downregulation of only one of these proteins reduces PCCs metabolic flexibility with the accumulation of FA-intermediate metabolites in the mitochondria. Together, our data implicate carnitine cycle as a primary regulator of adaptive metabolic reprogramming in PCCs and suggest new potential druggable pathways for prevention and treatment of prostate cancer.

INTRODUCTION

Cancer cells reprogram their metabolic pathways, including glycolysis, the Krebs cycle and fatty acid (FA) metabolism, to satisfy their need to proliferate, survive and metastasize.[1–3] This altered metabolism is a common denominator among heterogenic malignant cells and has been identified as one of the hallmarks of cancer.

Tumor cells proliferation is supported by aerobic glycolysis in which pyruvate is transformed into lactate independently of the presence of oxygen (Warburg effect), and not by fatty acid oxidation (FAO), the primary source of energy production in normal cells.

Additional metabolic peculiarities of tumor cells are the high rate of glutamine oxidation and the increase of FA synthesis. This reorganization of cancer metabolism is fundamental to satisfy the energy as well as the biosynthetic intermediate request of proliferating cells and to preserve the integrity of the cells from the harsh and hypoxic environment.[4–7]

However, although FA synthesis is within a clear metabolic framework, the extent of the role of FA catabolism, as the energy and materials sources for cancer proliferation, is still being deciphered.

A particularly intriguing example of how FAs have potential to fuel tumor cells occurs with prostate cancer. The metabolism of the normal prostate cells is changed greatly upon transformation.[8–10]

The normal prostate cells have a truncated Krebs cycle where the neo-synthesized citrate is a secretory product rather than an intermediate of metabolism. Thus, in the prostate, the ATP production derives via aerobic glycolysis, with less dependence on aerobic oxidation.

An increase in oxidative phosphorylation is a requirement for the progression of the prostate tumor, and so a continuous supply of acetyl-CoA is required to ensure citrate oxidation via the Krebs cycle.[11,12] As prostate cancer cells (PCCs) exhibit a low rate of glycolysis, FAO serves as the main source of acetyl-CoA, and by extension, ATP (Figure 1).[13–15]

The need for lipids of prostate neoplastic tissue can be satisfied by several mechanisms.[16] The uptake of circulating lipids and the transfer of FA from stromal adipocytes to PCCs increase *de novo* synthesis of lipids and phospholipids, and accumulation of cholesteryl ester as cytosolic lipid droplets.[16] Unlike this metabolic reprogramming, alterations in lipid-associated pathways encountered in prostate cancer remain ill-defined.

FAs used as energy substrate require ~25 different enzymes and transport proteins, which carry out the cellular uptake and activation of FAs, their translocation into the mitochondrial matrix, and their β-oxidation. In particular, the mitochondrial inner

[1]Institute of Agro-environmental and Forest Biology, National Research Council, IBAF – CNR, Naples, Italy; [2]Institute of Bioscience and BioResources – CNR, Naples, Italy; [3]Department of Molecular Biotechnology and Health Sciences, Laboratory of Immunology, University of Turin, Turin, Italy; [4]Prostate Cancer Unit, Department Urology, University 'Sapienza', Policlinico Umberto I, Rome, Italy and [5]Department of Experimental Medicine, Biotechnology and Molecular Biology Section, University of Campania 'Luigi Vanvitelli', Naples, Italy. Correspondence: Professor G Peluso, Institute of Agro-environmental and Forest Biology, National Research Council, IBAF – CNR, via P. Castellino,111, Naples, Italy.
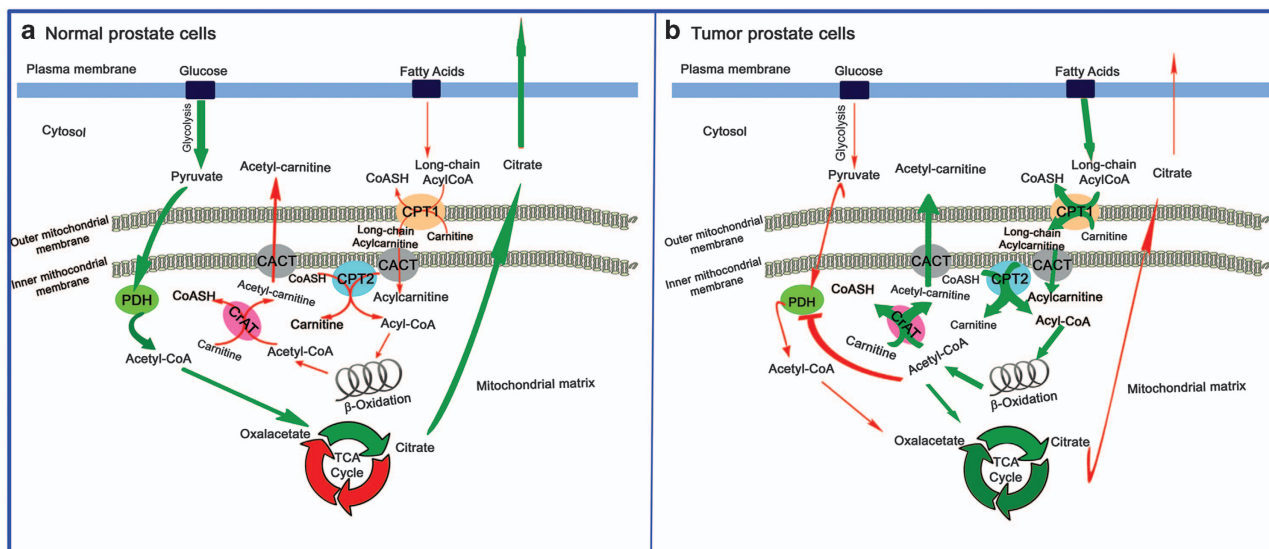E-mail: gianfranco.peluso@ibaf.cnr.it

Figure 1. Schematic representation of metabolic differences between normal and cancer prostate cells. (**a**) In normal prostate cells, ATP is obtained mainly via glycolytic pathway and citrate is an end-product of glucose metabolism, rather than an utilizable intermediate. The truncated Krebs cycle allows to synthesize citrate from acetyl-CoA and oxaloacetate and to export citrate from the mitochondria to the cytosol by the mitochondrial citrate transporter. (**b**) In cancer prostate cells, FAO is the dominant bioenergetic pathway, and the carnitine cycle regulates the FA mitochondrial import/export, and the intra-mitochondrial acyl-CoA pools. Three components of the carnitine system (CPT1, CACT and CrAT) are upregulated in prostate cancer cells and work closely together to ensure mitochondrial FA supply and to avoid the mitochondrial side effects of FA overloading (that is, intra-mitochondrial accumulation of FAO intermediates). The intra-mitochondrial acetyl-CoA increase, imposed by the heavy lipid load, allosterically inhibits PDH that catalyzes the rate-limiting oxidative decarboxylation of pyruvate into acetyl-CoA. (FAO, fatty acid oxidation; FA, fatty acid; PDH, pyruvate dehydrogenase complex; CPT1, carnitine-palmitoyltransferase-1; CACT, carnitine-acylcarnitine translocase; CrAT, carnitine acetyltransferase. Green arrows: dominant metabolic pathway).

membrane is impermeable to fatty acyl-CoA thioesters and, thus, a specific system for transporting FAs across mitochondrial membranes has evolved.[17] The most important limiting steps of beta-oxidation is represented by a group of four carnitine acyltransferases, which govern FA mitochondrial import/export and regulate intra-mitochondrial acyl-CoA pools.[18]

It is known that the transport of long-chain FAs across the mitochondrial membrane depends on a complicated mechanism regulated by the carnitine system. Components of the carnitine systems are both enzymes able to catalyze the acyl-CoA +carnitine ↔ CoA+acylcarnitines reaction and carrier(s) involved in the bi-directional transport of acyl moieties from cytosol to mitochondria and *vice-versa*. The long-chain FA-CoA are converted into the carnitine derivatives by carnitine-palmitoyltransferase-1 (CPT1), an integral protein located on the outer mitochondrial membrane of the contact sites.[19] Acylcarnitines are transported into the mitochondrial matrix by carnitine-acylcarnitine translocase (CACT), that also exports by-products of FAO, such as acetylcarnitines, from mitochondria to cytosol.[20] In the mitochondrial matrix, long-chain acylcarnitines are reconverted to the respective long-chain acyl-CoAs by carnitine-palmitoyltransferase-2 (CPT2).[19] Finally, the enzyme carnitine acetyltransferase (CrAT) catalyzes the addition or the removal of carnitine from acetyl-CoA, promoting the efflux of two carbon acetyl units from mitochondria to cytosol and buffering the intra-mitochondrial pools of acetyl-CoA.[21] Despite the important role that the carnitine system can play in cancer cell metabolism, little is known about the expression level of each and every component of the system in cancer cells. Also, only scattered information is available about the epigenetic control of carnitine system related-gene expression in tumors, although there is evidence that microRNAs (miRNAs) can modulate the expression of CPT1 or CACT in normal cells undergoing metabolic stress condition (Figure 1).[22–25]

In the present study, we examined, in three prostate cell lines, PNT2 (prostate control cells), LNCaP (androgen-dependent PCCs) and PC3 (androgen-independent PCCs), the expression and

biological significance of all the components of the carnitine system. We first demonstrated that malignant prostate cells increase both expression and activity of some components of the carnitine system, specifically CPT1A, CACT and CrAT. Next, we provided, for the first time, evidence that the overexpression of these proteins is regulated by the concordant decrease of specific miRNAs (hsa-miR-124-3p, hsa-miR-129-5p and hsa-miR-378) in both LNCaP and PC3 cells, regardless of their hormone sensitivity. Of interest, we demonstrated that control of the carnitine system by miRNAs is present also in prostate tissue specimens obtained from patients suffering from prostate cancer.

Our results give oncogenic relevance to the carnitine system and underline the biological role of the carnitine cycle in the maintenance of cancer metabolic flexibility. Therefore, the evaluation of CPT1A/CACT/CrAT proteins could provide additional predictive markers over conventional analysis in prostate cancer. Finally, these findings may suggest new druggable pathways for prevention and treatment of prostate cancer.

RESULTS

Carnitine system in prostate cells

Enhanced mitochondrial β-oxidation of FAs, such as palmitate, has been linked to tumor promotion in prostate cancer.[13,14,26] Indeed, we observed higher oxidation rate of palmitate in PC3 cells than in PNT2 cells, supporting that PCCs promote FAO as the dominant pathway to meet tumor bioenergetic requirements (Figure 2a).

To investigate whether increased β-oxidation was related to an increased flux of FAs into the mitochondria via changes in key carrier levels, we analyzed the expression (both at mRNA and protein levels) as well as the activity of CPT1, CPT2, CACT and CrAT.

As shown in Figure 2b, mRNA expression levels of *CPT1A*, *CACT* and *CRAT* were significantly upregulated in PC3 respect to PNT2
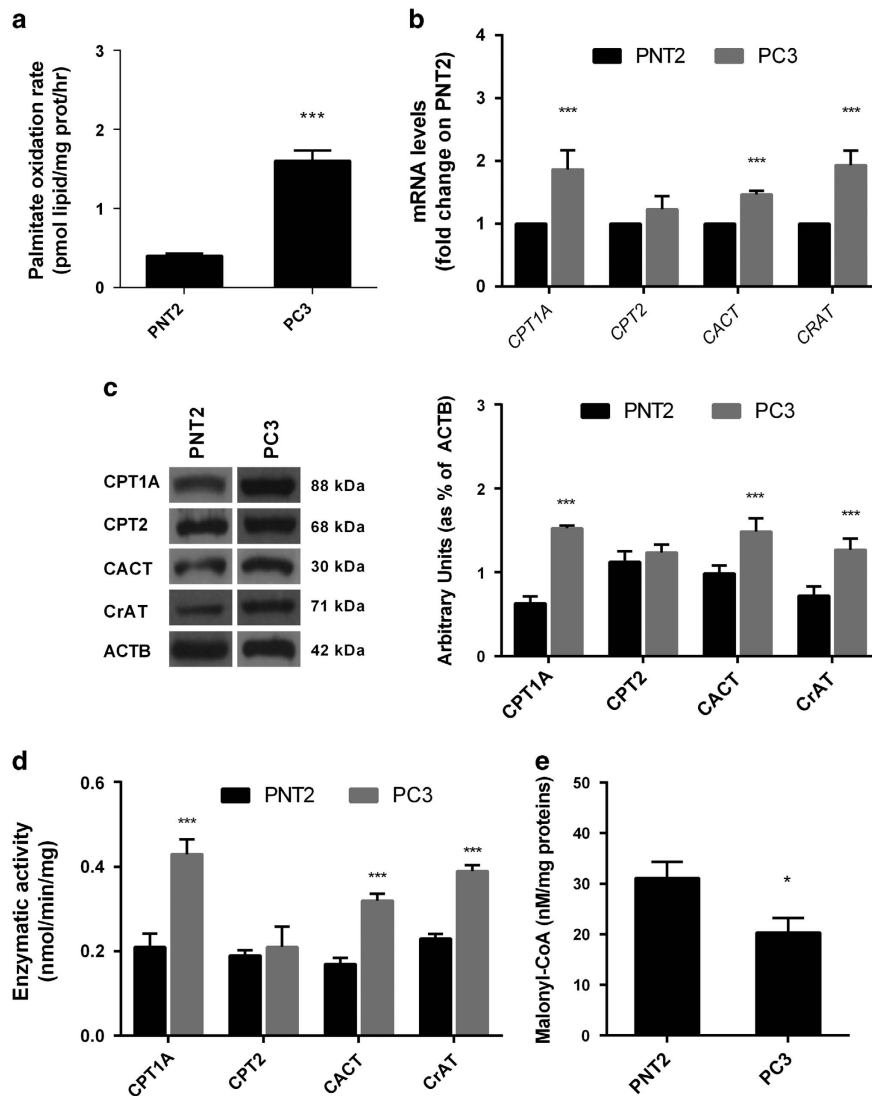
Figure 2. FAO and carnitine system analysis in PNT2 and PC3 cells. (**a**) Palmitate oxidation determined as [$^{14}CO_2$] production was measured in mitochondrial-enriched fractions. All values were normalized to the mitochondrial protein content and data expressed as mean $\pm$ s.d. ($n = 3$). (**b**) CPT1A, CPT2, CACT and CRAT mRNA levels were determined by quantitative real-time PCR and normalized to the housekeeping β-actin (ACTB). The comparative cycle threshold (CT) method ($2^{-\Delta\Delta CT}$) was applied to calculate relative differences in PCR results. (**c**) Western blot analysis of CPT1A, CPT2, CACT, CrAT and ACTB. Densitometric analyses were performed using Quantity One 1-D analysis software (BioRad, Italy). (**d**) The enzymatic activities were determined in mitochondria as described in materials and methods section and normalized for the mitochondrial protein contents. (**e**) Malonyl-CoA level was measured in PNT2, and PC3 cells and values were normalized to total protein content. The bars represent the means $\pm$ s.d. ($n = 6$). Statistically significant variations: *$P < 0.05$, **$P < 0.01$, ***$P < 0.005$ versus PNT2.

cells ($P < 0.05$), whereas no statistically significant difference was observed for CPT2 expression. Western blot analysis confirmed that CPT1A, CACT and CrAT proteins were markedly more expressed in tumor cell lines than in normal prostate cell line (Figure 2c).

To evaluate whether the observed increased expression of CPT1A, CACT and CrAT could be consistent with a gain of function of these proteins, enzyme activities were assayed. As showed in Figure 2d, we demonstrated that the activities of CPT1A, CACT and CrAT were markedly higher in PC3 mitochondria than in control PNT2 mitochondria.

To sustain an enhanced FAO, PCCs have to maintain a low level of malonyl-CoA, the CPT1A physiological allosteric inhibitor. Therefore, we analyzed the malonyl-CoA concentration in all cell lines and demonstrated that the amount of malonyl-CoA was significantly lower ($P < 0.05$) in malignant cells than in PNT2 cells (Figure 2e).

miRNAs expression in prostate cell lines

Recent studies highlighted the pivotal role of miRNAs in the finely post-transcriptional adjustment of enzymes involved in metabolic reprogramming of cancer cells.[27,28] Our preliminary examination of the miRNAs content in malignant and normal prostate cells with Small RNA App (CORE App in Illumina BaseSpace cloud), showed a very different overall content of RNA fragments (Supplementary Figure S1a) corroborated by the differential expression analysis. In particular, DESeq2 detected a total of 417 miRNAs differentially expressed using as threshold |log2(PC3/PNT2)| $\geqslant 1$ and FDR $\leqslant 0.1$ (Supplementary Figure S1b).[29] A more rigorous analysis, |log2(PC3/PNT2)| $\geqslant 3.5$, P-value $\leqslant 10^{-5}$ and FDR $\leqslant 0.1$, revealed a total of 80 miRNAs differentially expressed in the PC3 compared with PNT2, including 32 miRNAs upregulated and 48 miRNAs downregulated (Supplementary Table S2).

Then, we selected three specific miRNAs (hsa-miR-129-5p, hsa-miR-124-3p and hsa-miR-378) identified by miRNA target
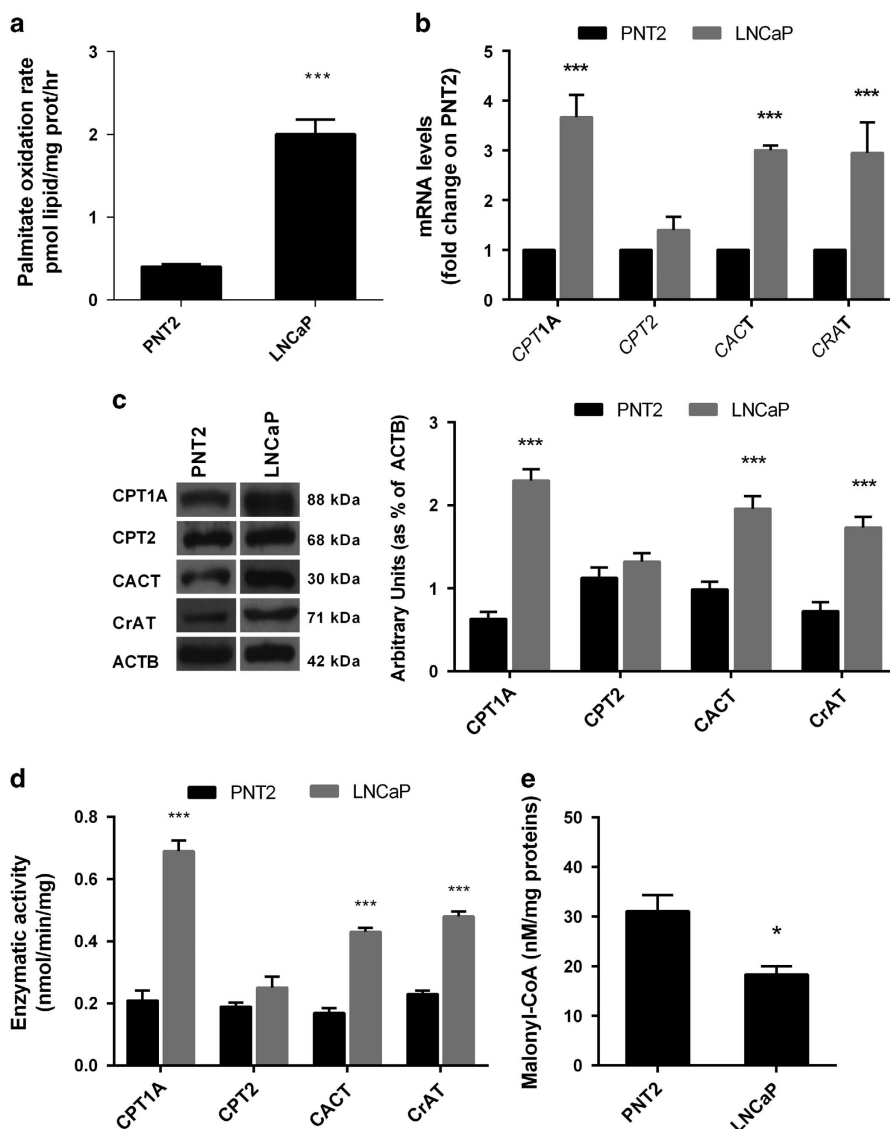
Figure 3. FAO and carnitine system analysis in LNCaP cells. (**a**) Palmitate oxidation determined as [$^{14}CO_2$] production was measured in mitochondrial-enriched fractions. All values were normalized to the mitochondrial protein content and data expressed as mean ± s.d. ($n = 3$). (**b**) CPT1A, CPT2, CACT and CRAT mRNA levels were determined by quantitative real-time PCR and normalized to the housekeeping β-actin (ACTB). The comparative cycle threshold (CT) method ($2^{-\Delta\Delta CT}$) was applied to calculate relative differences in PCR results. (**c**) Western blot analysis of CPT1A, CPT2, CACT, CrAT and ACTB. Densitometric analyses were performed using Quantity One 1-D analysis software (BioRad, Italy). (**d**) The enzymatic activities were determined in mitochondria as described in materials and methods section and normalized for the mitochondrial protein contents. (**e**) Malonyl-CoA level was measured in PNT2, and LNCaP cells and values were normalized to total protein content. The bars represent the means ± s.d. ($n = 6$). Statistically significant variations: *$P < 0.05$, **$P < 0.01$, ***$P < 0.005$ versus PNT2.

prediction algorithms as possible intermediaries in the regulation of carnitine cycle proteins. Web-based tools identified CACT as a target of hsa-miR-129-5p (downregulated by 4.9-fold in PC3 respect to PNT2), CPT1A as a target of hsa-miR-124-3p (down-regulated by 3.5-fold) and CRAT as a target of hsa-miR-378 (downregulated by 3.5-fold). Indeed, sequence analysis revealed that the 3′-untranslated region (UTRs) of CACT, CPT1A and CRAT contain the putative binding site for the identified miRNAs (Supplementary Figure S2).

CPT1A, CACT and CrAT are direct targets of hsa-miR-124-3p, hsa-miR-129-5p and hsa-miR-378

To determine whether the carnitine system deregulation was a common signature in prostate cancers, we analyze the palmitate oxidation rate and the expression both at the transcriptional and translational level of CPT1A, CACT and CRAT in LNCaP, a well-known model of androgen-dependent PCC line. As shown in Figure 3, LNCaP exhibited, respect to PNT2, a markedly upregulation of CPT1A, CACT and CrAT at mRNA (Figure 3b) and protein levels (Figure 3c) and an increased β-oxidation (Figure 3a). Functional assays and malonyl-CoA determination corroborated these results showing an overall increase in enzymatic activity (Figure 3d) and a decrease of malonyl-CoA concentration (Figure 3e).

Next, to validate miRNAs sequencing in both the androgen-independent (PC3) and androgen-dependent (LNCaP) prostate tumor cells, the endogenous levels of identified miRNAs were analyzed by TaqMan-based quantitative real-time PCR (qPCR). Consistent with bioinformatic analysis, a statistically significant downregulation of hsa-miR-129-5p, hsa-miR-124-3p and hsa-miR-378 was evident in both tumor cells compared with PNT2 (Figure 4a).
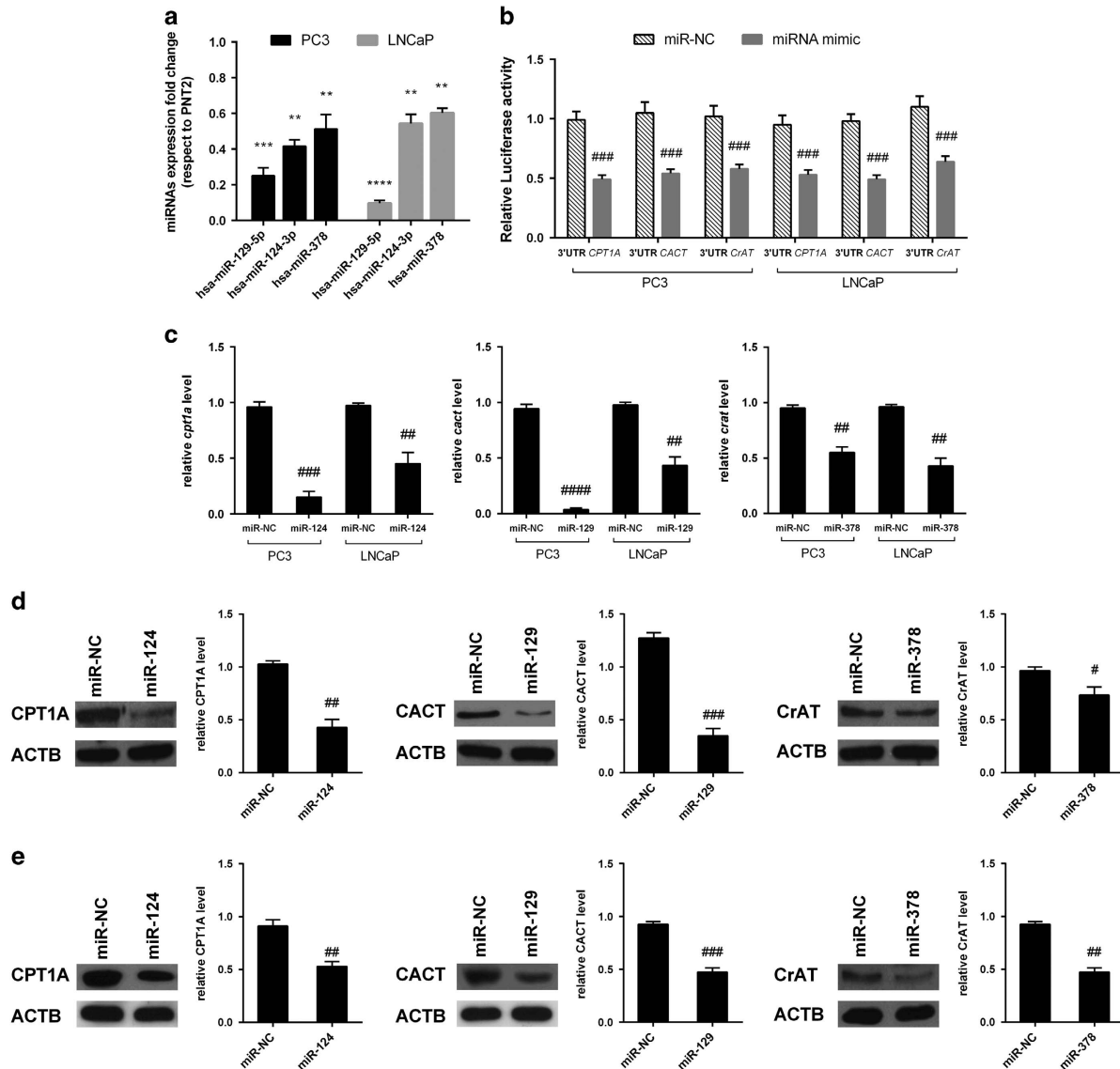
Figure 4. Validation of CPT1A, CACT and CrAT as targets of miR-124, miR-129 and miR-378 in PC3 and LNCaP cells. (**a**) qPCR validation of differentially expressed miRNAs in PC3 and LNCaP respect to PNT2. Detection of miRNAs was performed by TaqMan qPCR miRNA assay and normalized to RNU6B. The comparative cycle threshold (CT) method ($2^{-\Delta\Delta CT}$) was applied to calculate relative differences in PCR results. (**b**) Luciferase reporter assays. PC3 and LNCaP cells were transfected with 3′-UTR-reporter constructs together with miRNA mimics. miR-NC was used as negative control, and the results were normalized to *Renilla* luciferase activity. (**c**) MiRNA targets levels were detected in PC3 and LNCaP cells by qPCR and normalized to *ACTB*. The comparative cycle threshold (CT) method (2-ΔΔCT) was applied to calculate relative differences in PCR results. Western blot analysis of CPT1A, CACT and CrAT proteins was performed on total protein fraction of PC3 (**d**) and LNCaP (**e**). The protein expression was normalized to the housekeeping protein ACTB. The bars represent the means ± s.d. ($n = 6$). Statistically significant variations: **$P < 0.01$, ***$P < 0.005$, ****$P < 0.001$ versus PNT2; #$P < 0.05$, ##$P < 0.01$, ###$P < 0.005$, ####$P < 0.001$ miRNAs versus miR-NC.

To verify if hsa-miR-129-5p, hsa-miR-124-3p and hsa-miR-378 directly bind with 3′ UTRs of *CACT*, *CPT1A* and *CRAT*, luciferase reporter assay was carried out. Each corresponding 3′-UTR sequence, inserted into a luciferase reporter plasmid, was co-transfected with miR-124, miR-129 or miR-378 into PC3 and LNCaP cells (Figure 4b). Our results demonstrated that the identified miRNAs significantly ($P < 0.005$) inhibited the activity of firefly luciferase confirming that *CPT1A*, *CACT* or *CRAT* mRNAs are direct the target of the corresponding miRNAs. Next, the effect of miRNA mimics overexpression on the mRNA and protein levels of identified targets was examined. The qPCR (Figure 4c) and western blot (Figures 4d and e) analyses showed that miR-129, miR-124 or miR-378 markedly suppressed the mRNA and protein

expression levels of CPT1A, CACT or CrAT, in comparison with miR-NC. Taken together, these findings suggest that hsa-miR-124-3p, hsa-miR-129-5p and hsa-miR-378 are involved in modulating, at the post-transcriptional level, the expression of CPT1A, CACT and CrAT in both PCC lines.

Anti-tumorigenic effects of identified miRNAs in PCCs
To evaluate the tumorigenic potential of PCCs overexpressing miR-124, miR-129 or miR-378, the proliferative cell rate, and the cell migration and invasive ability were analyzed on PC3, and LNCaP transfected with miRNA mimics as well as miR-NC (Figures 5 and 6). The MTT proliferation test demonstrated that overexpression of each miRNA mimics was able to decrease
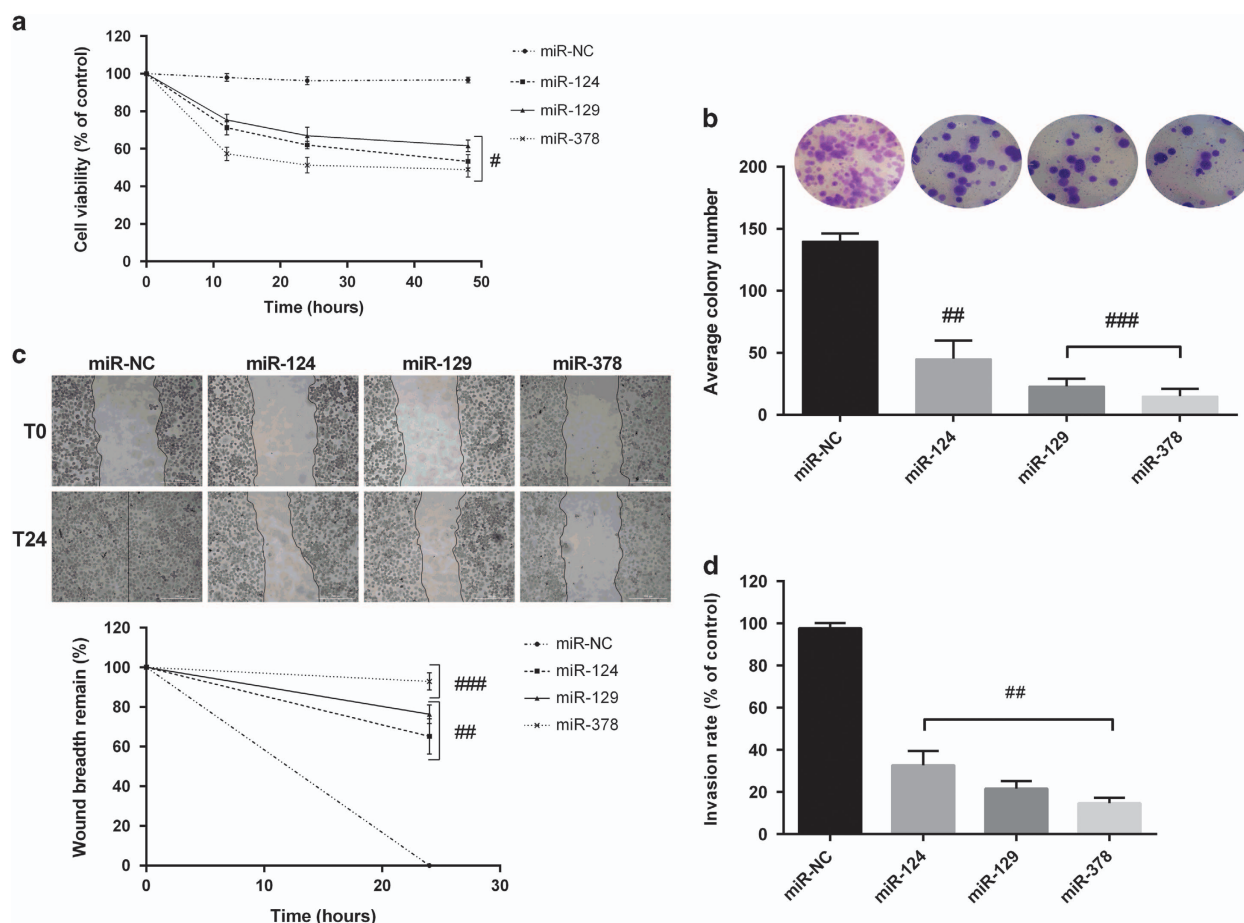
Figure 5. Influence of forced expression of miR-124, miR-129 and miR-378 on PC3 proliferation, migration and invasion. (**a**) Cell proliferation of PC3 cells was determined by MTT assay after 12, 24 and 48 h. (**b**) Colony formation assay was performed after 14 days of culture. For quantification colonies with at least 50 cells were considered. Representative micrographs were obtained using phase contrast microscope after staining with crystal violet. (**c**) Wound-healing assay was performed on transfected PC3 cells, and the wound closure rate was measured by detecting the closure distance after 24 h. Representative micrographs of the cell migration (up) and quantification (down) from three independent experiments were presented. (**d**) Transwell invasion assay with Matrigel was performed in mimics or miR-NC transfected PC3 cells after 24 h. Five random fields in each well were counted under a microscope. The bars represent the means ± s.d. ($n = 6$). Statistically significant variations: [#]$P < 0.05$, [##]$P < 0.01$, [###]$P < 0.005$ miRNAs versus miR-NC.

significantly ($P < 0.05$) PC3 and LNCaP cell growth (Figures 5a and 6a). The colony formation assay, which reflects the self-renewal ability of transfected cells, also showed that the gain of function of miR-124, miR-129 or miR-378 reduced prostate cancer colony formation (Figures 5b and 6b).

As assessed by a wound-healing assay (Figure 5c), the migration capability of PC3 cells was significantly inhibited by the over-expression of miR-124 (65%, $P < 0.01$), miR-129 (75%, $P < 0.01$) and miR-378 (93%, $P < 0.005$). Moreover, the number of PC3 cells crossed Matrigel was markedly decreased by 85–70% compared with the control cells (Figure 5d).

Similarly, forced expression of miR-124, miR-129 or miR-378 in LNCaP cells negatively modulate migration and invasion (Figures 6c and d). In particular, the wound gap was >93%, and the number of cells migrating to the lower chamber decreased by >80% after each miRNA mimics transfection in comparison with miR-NC transfection. To further validate the regulatory role of miRNAs on the identified targets expression, rescue experiments were performed in both cell lines. The transient transfection of exogenous CPT1A, CACT or CrAT lacking their 3'UTR with each mimic, rescued tumorigenic potential of PCCs (Supplementary Figure S3 and S4) confirming the regulatory role of miRNAs on the identified targets expression.

Overexpression of miR-124, miR-129 and miR-378 modulates mitochondrial FA flux modifying intracellular acylcarnitine contents

Tumor cells can rapidly switch between fat and glucose oxidation exhibiting a metabolic flexibility in response to nutrients availabilities.[30] These raises the question of whether upregulated carnitine cycle is responsive to fluctuations in the nutrient state. As shown in Figures 7a and b, PC3 and LNCaP cancer cells exhibited, also in the presence of pyruvate concentration up to 0.2 mM, a significant increase of [1-^{14}C]palmitate oxidation when compared with PNT2 control cells.

Next, to provide an index of how the PCCs metabolically respond to carnitine cycle perturbation induced by overexpression of each miRNA, the evaluation of both ASAC (acid-soluble, short and medium chains) and AIAC (acid-insoluble, long-chains) acylcarnitines content in miRNAs transfected PC3 and LNCaP cells was determined (Figures 7c and d). Forced expression of miR-129 or miR-378 induced a significant increase ($P < 0.005$) in AIAC content in both cancer cell lines respect to miR-NC transfected cells. On the contrary, the downregulation of CPT1A expression by miR-124, limiting the conversion of long-chain acyl-CoA moieties to long-chain acylcarnitine, led to a significant decrease ($P < 0.005$) in AIAC content. Moreover, miR-124 and miR-129 overexpressing cells did not exhibit any significant difference in
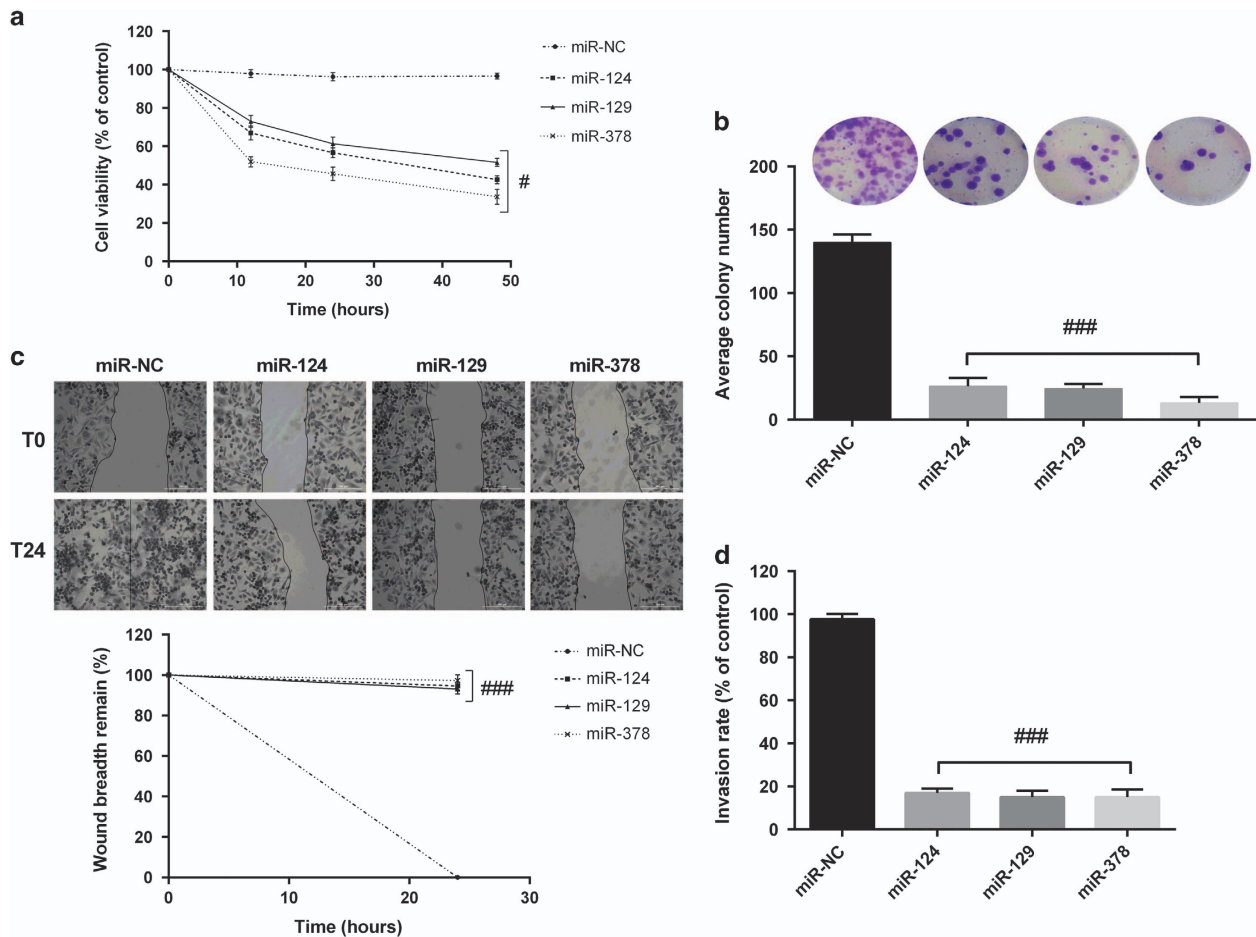
Figure 6. Influence of forced expression of miR-124, miR-129 and miR-378 on LNCaP proliferation, migration and invasion. (**a**) Cell proliferation of LNCaP cells was determined by MTT assay after 12, 24 and 48 h. (**b**) Colony formation assay was performed after 14 days of culture. For quantification colonies with at least 50 cells were considered. Representative micrographs were obtained using phase contrast microscope after staining with crystal violet. (**c**) Wound-healing assay was performed on transfected LNCaP cells, and the wound closure rate was measured by detecting the closure distance after 24 h. Representative micrographs of the cell migration (up) and quantification (down) from three independent experiments were presented. (**d**) Transwell invasion assay with Matrigel was performed in mimics or miR-NC transfected LNCaP cells after 24 h. Five random fields in each well were counted under a microscope. The bars represent the means ± s.d. ($n = 6$). Statistically significant variations: $^{\#}P < 0.05$, $^{\#\#}P < 0.01$, $^{\#\#\#}P < 0.005$ miRNAs versus miR-NC.

ASAC content in comparison with control miR-NC transfected cells, while the transfection with miR-378 led to a relevant ASAC reduction.

Taken together, these results suggest that the FA addiction of PC3 and LNCaP cells is conferred by the constitutive upregulation of the carnitine cycle, and that inhibition of CPT1A, CACT or CrAT expression blocks the ability of PCCs to completely metabolize lipid substrates, leading to abnormal cell acylcarnitine profiles.

miRNAs overexpression in tissue specimens of prostate cancer

Owing to the highly heterogeneous nature of prostate cancer, a laser capture microdissection microscope was used on 30 FFPE prostatectomy. Laser capture microdissection allows to determine the densest region of tumor and capture as much tumor RNA as possible enriching for malignant glands and avoiding contamination with stromal tissue or non-malignant glands. The expression of the identified miRNAs and their targets in laser capture samples was analyzed by qPCR. As shown in Figures 8a–c, a significantly decreased expression ($P < 0.001$) of hsa-miR-129-5p, hsa-miR-124-3p and hsa-miR-378 was observed in all of the tumor samples compared with normal controls, demonstrating the same down-regulation identified in PCCs. Moreover, *CPT1A*, *CACT* and *CRAT*

expression levels (Figure 8d-f) were significantly ($P < 0.001$) upregulated in all the tumor samples respect to controls.

DISCUSSION

The complex molecular events that govern FA metabolic pathway (s) during prostate cancerogenesis are largely unknown. Here, we report that in PCCs, hsa-miR-129-5p, hsa-miR-124-3p and hsa-miR-378 downregulation greatly contribute to deregulation of mitochondrial FAO. We clarify how miRNAs perturbation of carnitine cycle promotes a novel metabolic adaptation of PCC to support cancer development and progression.

In the last few years, systematic profiles detailing the miRNA expression in prostate cancer vs normal prostate cells have demonstrated both up- and downregulated miRNA patterns.[31–33] However, the results of these studies were highly contradictory, and their discrepancies may be explained by differences in tissue selection, RNA and the platforms used for the detection.[34] Moreover, Gill *et al*.[35] highlighted the need for seeking an accurate link between miRNAs and prostate cancer through an understanding of the signaling pathways that these miRNAs control, to identify therapeutically attractive molecular targets.

At our knowledge, only one paper has analyzed the regulation of lipogenesis and cholesterogenesis by miRNA in prostate tumor

cells, while no information is available in the scientific literature about the epigenetic control of FAO-associated genes in prostate cancer.[36]

For the first time, we demonstrated that hsa-miR-124-3p, hsa-miR-129-5p and hsa-miR-378 regulated CPT1A, CACT and CrAT expression in PCCs, regardless of their hormone sensitivity.
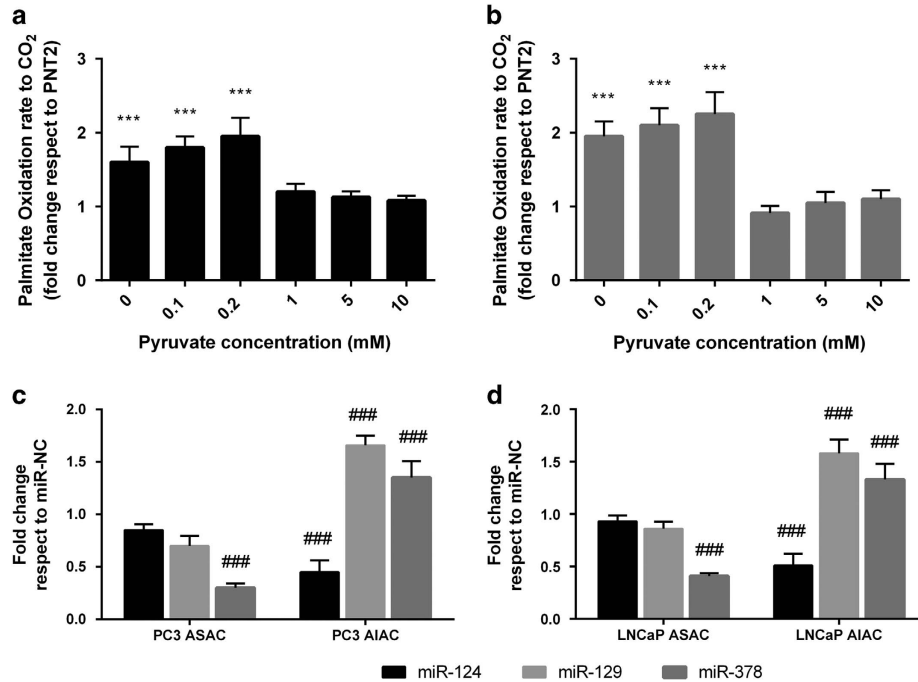

Figure 7. Evaluation of prostate cancer cell FA metabolism. The [1-^{14}C]palmitate oxidation rate in PC3 (**a**) or LNCaP (**b**) cells was measured in the presence of different concentration of pyruvate (0–10 mM). All values were normalized to the mitochondrial protein content, and results are reported as fold change respect to PNT2 oxidation rates. Acid-soluble (ASAC) and acid-insoluble (AIAC) acylcarnitines content was determined by the radioisotopic method in transfected PC3 (**c**) and LNCaP (**d**) cells. Results are reported as fold change respect to miR-NC transfected cells. The bars represent the means ± s.d. ($n = 6$). Statistically significant variations: ***$P < 0.005$ versus PNT2; ###$P < 0.005$ miRNAs versus miR-NC.
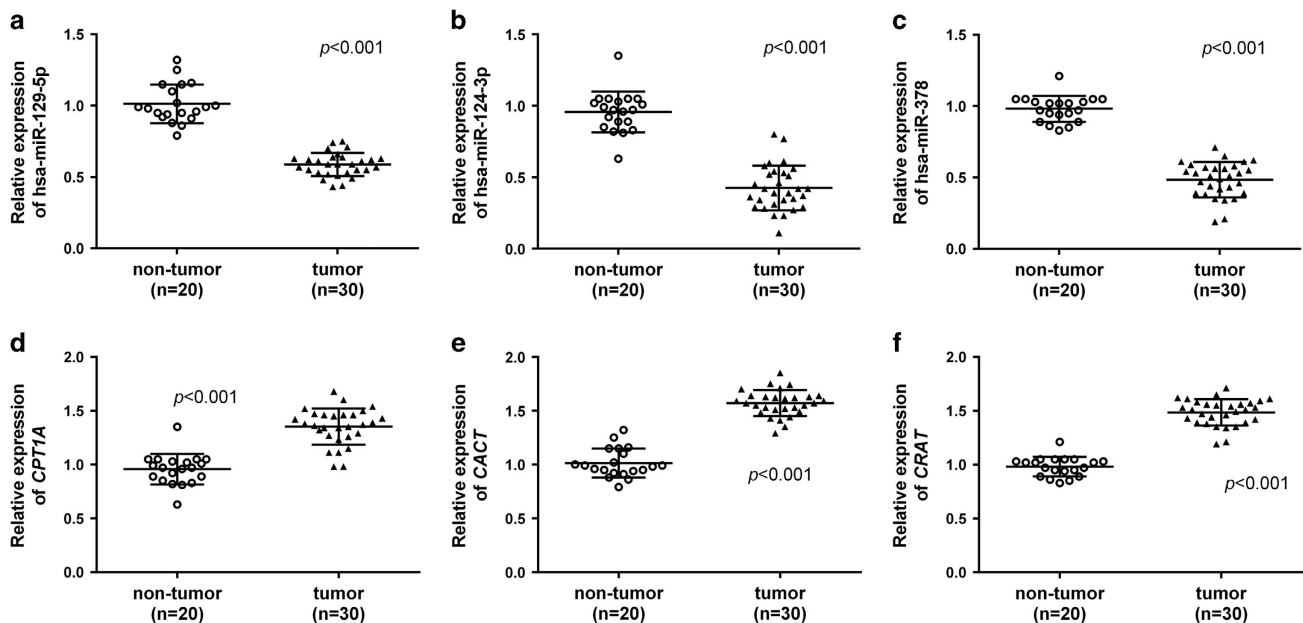

Figure 8. Expression of identified miRNAs in laser capture samples of prostate cancer. (**a**) hsa-miR-129-5p, (**b**) hsa-miR-124-3p and (**c**) hsa-miR-378 expression levels were detected in 30 formalin-fixed-paraffin-embedded (FFPE) prostatectomy tissue and in 20 FFPE normal epithelial tissue samples after LCM. Detection of miRNAs was performed by TaqMan qPCR miRNA assay and normalized to RNU6B. The relative differences were calculated using the 2$^{-\Delta Ct}$ method. (**d**) CPT1A, (**e**) CACT and (**f**) CRAT mRNA levels were determined by quantitative real-time PCR and normalized to the housekeeping β-actin (ACTB). The comparative cycle threshold (CT) method (2-$\Delta\Delta$CT) was applied to calculate relative differences in PCR results. The bars represent the means ± s.d.

miR-124 is known to function as a tumor suppressor in many cancers.[37,38] Shi et al.[39] demonstrated that miR-124 downregulation was a hallmark of malignant prostatic cells, and could contribute to the pathogenesis of prostate cancer. Our study suggests a new fundamental role for miR-124 in modulating CPT1A expression in PCCs. This overexpression, associated with an increased activity of CPT1A seems to be apparently in contrast with the lipogenic activity normally exacerbated in prostate cancer. In general, FA synthesis and FAO are mutually exclusive metabolic pathways, under the control of malonyl-CoA, an intermediate in FA synthesis. Malonyl-CoA acts as an allosteric inhibitor of CPT1 preventing FA biosynthesis and FAO from occurring simultaneously.[40] Surprisingly, we demonstrated that the amount of malonyl-CoA was extremely low in PCCs, indicating that the high rate of FA synthesis keeps a low level of malonyl-CoA. Thus, the overexpression of CPT1A, together with the loss of allosteric inhibition by malonyl-CoA, imposes a heavy lipid load on prostate cancer mitochondria.

miR-129-5p is deregulated in several tumors, such as laryngeal cancer, neuroendocrine tumors, gastric cancer and medullary thyroid carcinoma.[41–44] Ma et al.[45] reported that low miR-129-5p expression was strongly correlated with cancer invasion, recurrence and poor survival in hepatocellular carcinoma. Here we identified CACT as a novel target of miR-129-5p in prostate cancer.

CACT overexpression coordinates both the import of acylcarnitines inside the mitochondrial matrix in exchange of free carnitine, contributing to the increased FAO and the export of excess FAO intermediates as carnitine derivatives, thus avoiding intra-mitochondrial accumulation of acyl units.[46]

Recent findings have reported that in breast cancer cells the expression of miRNA-378 results in a shift from aerobic oxidative metabolism to glycolytic metabolism in the presence of available oxygen (Warburg effect) as represented by an increase in lactate levels and a reduction in oxygen consumption.[47] Thus, miRNA-378 counterbalances the metabolic actions of PGC-1β that orchestrates cellular programs of oxidative metabolism, by regulating the biogenesis of mitochondria and controlling the enzymes involved in oxidative phosphorylation.[48] Interestingly, it was found that CrAT is repressed by miR-378.[49] As CrAT decreases acetyl-CoA and regenerates free CoA, chronic inhibition of CrAT expression by miRNA-378 has the potential to raise the mitochondrial acetyl-CoA/CoA ratio to a level that promotes pyruvate dehydrogenase phosphorylation inhibiting glucose oxidation.[50] Conversely, in our study, we demonstrate that in PCCs miRNA-378 was downregulated leading to a concomitant increase of CrAT. Such high amounts of CrAT, which essentially siphons acetyl-CoA from the TCA cycle, are not in contrast with the FA-dependent metabolism of PCCs. Besides, the conversion of short-chain acyl-CoAs to their acylcarnitine counterparts by CrAT permits a CACT-dependent export of acyl moieties from mitochondria to cytosol avoiding both accumulations of FA-intermediate metabolites in the mitochondria and perturbation of FAO.[51]

A mechanistic explanation of these results might be that the induced overexpression of CPT1A, CACT and CrAT, the key players of carnitine cycle, contribute to maintaining a high metabolic flexibility of PCCs. We also demonstrated that forcing miR-124-3p, miR-129-5p or miR-378 expression in PCCs significantly decreased migration, proliferation and invasion of transfected cells. Our evaluation of acylcarnitines content and palmitate oxidation degree in cancer cells has provided a measure of how PC3 and LNCaP metabolically respond to carnitine cycle perturbation induced by overexpression of each miRNA.

Finally, we analyzed human prostate cancer samples and prostate control specimens, and we confirmed that the aberrant expression of miR-124-3p, miR-129-5p and miR-378 as well as CPT1A, CACT and CrAT overexpression were present also in primary tumors. Together, our data implicate carnitine cycle as a primary regulator of adaptive metabolic reprogramming in PCCs and suggest new potential druggable pathways for prevention and treatment of prostate cancer.

MATERIALS AND METHODS
For details, see Supplementary Materials and Methods.

Materials
The human CPT1A, CACT and CRAT sequences cloned in the pCMV6-XL5 expression vector with or without their 3′ UTR were purchased from OriGene Technologies (Rockville, MD, USA). All chemical reagents were of analytical grade or higher and were from Sigma-Aldrich (Milan, Italy).

Cell culture
The human prostate adenocarcinoma cell lines (PC3 and LNCaP), and the immortalized non-cancerous prostate epithelial cell line (PNT2),[52,53] were purchased from the European Collection of Cell Cultures (ECACC, UK) and tested for mycoplasma contamination. Cells were grown according to the manufacturer's instructions (with an approximate population doubling time of 31 h for PC3 and 38 h for LNCaP) and used within 2–4 months.

Malonyl-CoA measurement
Malonyl-CoA concentration was quantified in whole-cell lysates from PNT2, PC3 and LNCaP cells and analyzed by enzyme-linked immunosorbent assay as reported by Fritz et al.[54]

Enzymatic determinations
CPT1A activity was assayed in prostate cell mitochondria as the incorporation of radiolabeled carnitine into acylcarnitine in the presence or absence of malonyl-CoA according to Giordano et al.[55] and Priore et al.[56] CPT1A activity insensitive to 100 mmol/l malonyl-CoA was always subtracted from the experimentally determined CPT1A activity. CACT activity was assayed according to Peluso et al. and IJlst et al.[57,58] CrAT activity was determined as described by Muoio et al.[59] Enzymatic activities were determined in at least three different experiments.

RNA isolation, reverse transcription and qPCR
Total RNA (mRNA and miRNAs) was extracted from cells using QIAzol reagent (Qiagen, Milan, Italy) according to the manufacturer's instructions. qPCR and data collection were performed on 7900HT Fast Real-time PCR System (Applied Biosystems, Milan, Italy).

miRNAs transient transfection
Cells were transfected by Lipofectamine RNAiMAX (Invitrogen, Milan, Italy) following manufacturer's protocol. hsa-miR-129-5p, hsa-miR-124-3p, hsa-miR-378 mirVana miRNA mimics (Ambion, Milan, Italy) and mirVana miRNA mimic negative control #1 (miR mimic NC, Ambion) were purchased from Applied Biosystems. For convenience, hsa-miR-129-5p, hsa-miR-124-3p, hsa-miR-378 mimic and the negative control were hereafter referred to as miR-124, miR-129, miR-378 and miR-NC, respectively. Forced expression of mimics was confirmed by qPCR, and transfected cells were used in further analyses. For rescue experiments, PC3 and LNCaP cells were co-transfected with 10 pmole of mimics and 50 ng of each vector.

Luciferase assay
The pEZX-MT06 target reporter vectors containing full length of CPT1A 3'UTR, CACT 3'UTR and CrAT 3'UTR inserted downstream of the firefly luciferase sequence, were purchased from GeneCopoeia (Rockville, MD, USA). Twenty-four hours before transfection, 1.5×10^4 cells were plated in a 96-well plate. Ten pmoles of miR-124, miR-129, miR-378 or miR-NC were transfected into cells together with 100 ng of pEZX-MT MT06 clones by Lipofectamine RNAiMAX. Luciferase assay was performed 24 h after transfection by the Luc-Pair Luciferase Assay Kit (GeneCopoeia). Sample firefly luciferase expression was normalized against Renilla luciferase activity.

Cell proliferation and Colony forming assay

Following transfection, cell proliferation at 0, 12, 24 and 48 h was determined by MTT assay following manufacturer's protocol (Sigma-Aldrich). A microplate reader (Cytation3, ASHI) was used to measure the absorbance of each well at 570 nm.

For colony formation assay, cells were counted, seeded in six-well plates (in triplicate) at a density of 500 cells/well and incubated at 37 °C in a 5% CO_2 humidified incubator. The culture medium was replaced every 3days. After 14 days in culture, cells were stained with crystal violet and counted. Colonies with at least 50 cells were considered for quantification. Representative plates were photographed using phase contrast microscope (Leica, Milan, Italy).

Cell migration and invasion assays

Approximately 1×10^5 cells were plated in two-well Lab-Tek Chamber Slide (Sigma-Aldrich). After overnight incubation, cells were transfected with mimics or miR-NC. Wounds were created in confluent cells using a 200 µl pipette tip. Any free-floating cells or debris were removed by rinsing cells several times with media, and the speed of wound closure was monitored after 24 h by measuring the distance of the wound from 0 h. Each experiment was conducted in triplicate, and representative scrape lines were photographed using phase contrast microscope (Leica).

For the invasion assays, after 24 h transfection, 1×10^5 cells were seeded onto the transwell migration chambers in serum-free media (8 µm pore size; Millipore, Milan, Italy). The membrane in the upper chamber was coated overnight with 1 mg/ml BD Matrigel Matrix (BD Biosciences, Milan, Italy). After 24 h, the non-invading cells were clear out with a cotton-tipped swab, and the cells at the bottom of the insert were stained with May-Grunwald-Giemsa (Sigma-Aldrich). Stained cells were counted under a microscope (Leica) at ×200 magnification of five random fields in each well. At least three independent experiments were performed.

Western blotting

Polyacrylamide gel electrophoresis was carried out, in triplicate, according to standard procedures using 30 µg of total cell lysates. Membranes were probed with the specific primary antibodies followed by secondary antibodies conjugated with horseradish peroxidase. The bands were quantified densitometrically using Quantity One 1-D analysis software (BioRad, Milan, Italy).

Energy substrate oxidation

Acid-soluble acylcarnitines and acid-insoluble acylcarnitines were measured by a radioisotope method as described by Brass & Hoppel[60] in transfected cells after 24 h of treatment with [^{14}C]carnitine.

Palmitate oxidation was determined as the capture of $^{14}CO_2$ from palmitate ([1-^{14}C]palmitate at 0.5 µCi/ml, 150 µM). The reaction mixture contained 100 sucrose mM, 10 mM Tris/HCl, 80 mM KCl, 1 mM $MgCl_2$, 2 mM L-carnitine, 0.1 mM malate, 2 mM ATP, 50 µM CoA, 1 mM dithiothreitol, 0.2 mM ethylenediaminetetraacetic acid and 0.5% bovine serum albumin. Reactions were performed for 60 min at 30 °C after addition of enriched mitochondrial fraction. One hundred µl of 2 M sulfuric acid was added to terminate the reaction, and the radioactivity of CO_2 (trapped in 200 µl of 1 M NaOH) was determined by liquid scintillation counting.

For the analysis of palmitate oxidation dependence from pyruvate, palmitate oxidation was determined as aforementioned in the presence of 0-10mM cold pyruvate, as described by Kim et al.[61]

Laser capture microdissection and RNA extraction

This study included 30 patients diagnosed with organ-confined disease (pT2), no lymph node involvement (N0), no metastasis (M0) and Gleason score >6 (3+3), who underwent a radical retropubic prostatectomy at the Prostate Unit, Department of Urology, Policlinico Umberto I, University Sapienza (Rome, Italy). Written informed consent was obtained from all of the patients before the study, and the protocol was approved by the internal ethical committee. The stage and the grade of all the cases were classified according to OMS 2004, and the 1997 UICC TNM, respectively.

The freshly collected tissues were formalin-fixed-paraffin-embedded and reviewed by an expert pathologist with the primary goal of determining the densest region of the tumor. Tumor sections cut at 5 microns were lightly stained with hematoxylin and eosin before microdissection with a laser capture microdissection microscope (Arcturus Laser Capture Microdissection, Applied Biosystems). RNA extraction was performed using the Qiagen AllPrep DNA/RNA FFPE Kit (Qiagen) as described by Shahabi et al.[62]

Statistical analysis

All quantitative data were presented as the mean ± s.d. Each experiment was performed at least six times. Statistical significance was evaluated using a t-test or one-way analysis of variance, followed by Bonferroni's test for multiple comparisons to determine statistical differences between groups. All the data were analyzed with the GraphPad Prism version 5.01 statistical software package (GraphPad, La Jolla, CA, USA).

AUTHOR CONTRIBUTIONS

Conception and design: G Peluso, A Valentino, A Calarco, A Di Salle. Development of methodology: A Valentino, M Finicelli, S Margarucci, A Calarco, A Di Salle, RA Calogero. Acquisition of data (provided animals, acquired and managed patients, provided facilities, etc.): A Sciarra, A Gentilucci. Analysis and interpretation of data (for example, statistical analysis, biostatistics, computational analysis): S Crispi, RA Calogero, A Valentino. Writing, review and/or revision of the manuscript: A Valentino, A Calarco, A Di Salle, U Galderisi, G Peluso. Study supervision: U Galderisi, G Peluso.

REFERENCES

1 Dang CV, Semenza GL. Oncogenic alterations of metabolism. Trends Biochem Sci 1999; 24: 68–72.
2 Dang CV. Links between metabolism and cancer. Genes Dev 2012; 26: 877–890.
3 Modica-Napolitano JS, Singh KK. Mitochondrial dysfunction in cancer. Mitochondrion 2004; 4: 755–762.
4 DeBerardinis RJ, Mancuso A, Daikhin E, Nissim I, Yudkoff M, Wehrli S et al. Beyond aerobic glycolysis: Transformed cells can engage in glutamine metabolism that exceeds the requirement for protein and nucleotide synthesis. Proc Natl Acad Sci 2007; 104: 19345–19350.
5 Semenza GL. HIF-1: upstream and downstream of cancer metabolism. Curr Opin Genet Dev 2010; 20: 51–56.
6 Shanware NP, Mullen AR, DeBerardinis RJ, Abraham RT. Glutamine: pleiotropic roles in tumor growth and stress resistance. J Mol Med (Berl) 2011; 89: 229–236.
7 DeBerardinis RJ. Is cancer a disease of abnormal cellular metabolism? New angles on an old idea. Genet Med 2008; 10: 767–777.
8 McDunn JE, Li Z, Adam KP, Neri BP, Wolfert RL, Milburn MV et al. Metabolomic signatures of aggressive prostate cancer. Prostate 2013; 73: 1547–1560.
9 Sreekumar A, Poisson LM, Rajendiran TM, Khan AP, Cao Q, Yu J et al. Metabolomic profiles delineate potential role for sarcosine in prostate cancer progression. Nature 2009; 457: 910–914.
10 Teahan O, Bevan CL, Waxman J, Keun HC. Metabolic signatures of malignant progression in prostate epithelial cells. Int J Biochem Cell Biol 2011; 43: 1002–1009.
11 Costello LC, Franklin RB. The intermediary metabolism of the prostate: a key to understanding the pathogenesis and progression of prostate malignancy. Oncology 2000; 59: 269–282.
12 Costello LC, Franklin RB. 'Why do tumour cells glycolyse?': from glycolysis through citrate to lipogenesis. Mol Cell Biochem 2005; 280: 1–8.
13 Liu Y. Fatty acid oxidation is a dominant bioenergetic pathway in prostate cancer. Prostate Cancer Prostatic Dis 2006; 9: 230–234.

14 Liu Y, Zuckier LS, Ghesani NV. Dominant uptake of fatty acid over glucose by prostate cells: a potential new diagnostic and therapeutic approach. *Anticancer Res* 2010; **30**: 369–374.

15 Schlaepfer IR, Glode LM, Hitz CA, Pac CT, Boyle KE, Maroni P et al. Inhibition of lipid oxidation increases glucose metabolism and enhances 2-Deoxy-2-[(18)F]Fluoro-D-glucose uptake in prostate cancer mouse xenografts. *Mol Imaging Biol* 2015; **17**: 529–538.

16 Wu X, Daniels G, Lee P, Monaco ME. Lipid metabolism in prostate cancer. *Am J Clin Exp Urol* 2014; **2**: 111–120.

17 Bastin J. Regulation of mitochondrial fatty acid beta-oxidation in human: what can we learn from inborn fatty acid beta-oxidation deficiencies? *Biochimie* 2014; **96**: 113–120.

18 Foster DW. The role of the carnitine system in human metabolism. *Ann N Y Acad Sci* 2004; **1033**: 1–16.

19 Bonnefont JP, Djouadi F, Prip-Buus C, Gobin S, Munnich A, Bastin J. Carnitine palmitoyltransferases 1 and 2: biochemical, molecular and medical aspects. *Mol Aspects Med* 2004; **25**: 495–520.

20 Ramsay RR, Gandour RD, van der Leij FR. Molecular enzymology of carnitine transfer and transport. *Biochim Biophys Acta* 2001; **1546**: 21–43.

21 Jogl G, Hsiao YS, Tong L. Structure and function of carnitine acyltransferases. *Ann N Y Acad Sci* 2004; **1033**: 17–29.

22 Calin GA, Croce CM. MicroRNA signatures in human cancers. *Nat Rev Cancer* 2006; **6**: 857–866.

23 Khanmi K, Ignacimuthu S, Paulraj MG. MicroRNA in prostate cancer. *Clin Chim Acta* 2015; **451**: 154–160.

24 Kurisetty VV, Lakshmanaswamy R, Damodaran C. Pathogenic and therapeutic role of miRNAs in breast cancer. *Front Biosci (Landmark Ed)* 2014; **19**: 1–11.

25 Liu X, Chen X, Yu X, Tao Y, Bode AM, Dong Z et al. Regulation of microRNAs by epigenetics and their interplay involved in cancer. *J Exp Clin Cancer Res* 2013; **32**: 96.

26 Price DT, Coleman RE, Liao RP, Robertson CN, Polascik TJ, DeGrado TR. Comparison of [18 F]fluorocholine and [18 F]fluorodeoxyglucose for positron emission tomography of androgen dependent and androgen independent prostate cancer. *J Urol* 2002; **168**: 273–280.

27 Arora A, Singh S, Bhatt AN, Pandey S, Sandhir R, Dwarakanath BS. Interplay Between Metabolism and Oncogenic Process: Role of microRNAs. *Transl Oncogenomics* 2015; **7**: 11–27.

28 Pinweha P, Rattanapornsompong K, Charoensawan V, Jitrapakdee S. MicroRNAs and oncogenic transcriptional regulatory networks controlling metabolic reprogramming in cancers. *Comput Struct Biotechnol J* 2016; **14**: 223–233.

29 Love MI, Huber W, Anders S. Moderated estimation of fold change and dispersion for RNA-seq data with DESeq2. *Genome Biol* 2014; **15**: 550.

30 Cardenas-Navia LI, Mace D, Richardson RA, Wilson DF, Shan S, Dewhirst MW. The pervasive presence of fluctuating oxygenation in tumors. *Cancer Res* 2008; **68**: 5812–5819.

31 Ambs S, Prueitt RL, Yi M, Hudson RS, Howe TM, Petrocca F et al. Genomic profiling of microRNA and messenger RNA reveals deregulated microRNA expression in prostate cancer. *Cancer Res* 2008; **68**: 6162–6170.

32 Porkka KP, Pfeiffer MJ, Waltering KK, Vessella RL, Tammela TL, Visakorpi T. MicroRNA expression profiling in prostate cancer. *Cancer Res* 2007; **67**: 6130–6135.

33 Song C, Chen H, Wang T, Zhang W, Ru G, Lang J. Expression profile analysis of microRNAs in prostate cancer by next-generation sequencing. *Prostate* 2015; **75**: 500–516.

34 Schaefer A, Jung M, Kristiansen G, Lein M, Schrader M, Miller K et al. MicroRNAs and cancer: current state and future perspectives in urologic oncology. *Urol Oncol* 2010; **28**: 4–13.

35 Gill BS, Alex JM, Navgeet, Kumar S. Missing link between microRNA and prostate cancer. *Tumour Biol* 2016; **37**: 5683–5704.

36 Li X, Chen YT, Josson S, Mukhopadhyay NK, Kim J, Freeman MR et al. MicroRNA-185 and 342 inhibit tumorigenicity and induce apoptosis through blockade of the SREBP metabolic pathway in prostate cancer cells. *PLoS One* 2013; **8**: e70987.

37 Dong P, Ihira K, Xiong Y, Watari H, Hanley SJ, Yamada T et al. Reactivation of epigenetically silenced miR-124 reverses the epithelial-to-mesenchymal transition and inhibits invasion in endometrial cancer cells via the direct repression of IQGAP1 expression. *Oncotarget* 2016; **7**: 20260–20270.

38 Wang X, Liu Y, Liu X, Yang J, Teng G, Zhang L et al. MiR-124 inhibits cell proliferation, migration and invasion by directly targeting SOX9 in lung adenocarcinoma. *Oncol Rep* 2016; **35**: 3115–3121.

39 Shi XB, Ma AH, Xue L, Li M, Nguyen HG, Yang JC et al. miR-124 and Androgen Receptor Signaling Inhibitors Repress Prostate Cancer Growth by Downregulating Androgen Receptor Splice Variants, EZH2, and Src. *Cancer Res* 2015; **75**: 5309–5317.

40 Eaton S. Control of mitochondrial beta-oxidation flux. *Prog Lipid Res* 2002; **41**: 197–239.

41 Shen N, Huang X, Li J. Upregulation of miR-129-5p affects laryngeal cancer cell proliferation, invasiveness, and migration by affecting STAT3 expression. *Tumour Biol* 2016; **37**: 1789–1796.

42 Dossing KB, Binderup T, Kaczkowski B, Jacobsen A, Rossing M, Winther O et al. Down-Regulation of miR-129-5p and the let-7 Family in Neuroendocrine Tumors and Metastases Leads to Up-Regulation of Their Targets Egr1, G3bp1, Hmga2 and Bach1. *Genes (Basel)* 2015; **6**: 1–21.

43 Shen R, Pan S, Qi S, Lin X, Cheng S. Epigenetic repression of microRNA-129-2 leads to overexpression of SOX4 in gastric cancer. *Biochem Biophys Res Commun* 2010; **394**: 1047–1052.

44 Duan L, Hao X, Liu Z, Zhang Y, Zhang G. MiR-129-5p is down-regulated and involved in the growth, apoptosis and migration of medullary thyroid carcinoma cells through targeting RET. *FEBS Lett* 2014; **588**: 1644–1651.

45 Ma N, Chen F, Shen SL, Chen W, Chen LZ, Su Q et al. MicroRNA-129-5p inhibits hepatocellular carcinoma cell metastasis and invasion via targeting ETS1. *Biochem Biophys Res Commun* 2015; **461**: 618–623.

46 Palmieri F, Pierri CL. Mitochondrial metabolite transport. *Essays Biochem* 2010; **47**: 37–52.

47 Eichner LJ, Perry MC, Dufour CR, Bertos N, Park M, St-Pierre J et al. miR-378(*) mediates metabolic shift in breast cancer cells via the PGC-1beta/ERRgamma transcriptional pathway. *Cell Metab* 2010; **12**: 352–361.

48 Riehle C, Abel ED. PGC-1 proteins and heart failure. *Trends Cardiovasc Med* 2012; **22**: 98–105.

49 Carrer M, Liu N, Grueter CE, Williams AH, Frisard MI, Hulver MW et al. Control of mitochondrial metabolism and systemic energy homeostasis by microRNAs 378 and 378*. *Proc Natl Acad Sci USA* 2012; **109**: 15330–15335.

50 Lu J, Tan M, Cai Q. The Warburg effect in tumor progression: mitochondrial oxidative metabolism as an anti-metastasis mechanism. *Cancer Lett* 2015; **356**: 156–164.

51 Schlaepfer IR, Rider L, Rodrigues LU, Gijon MA, Pac CT, Romero L et al. Lipid catabolism via CPT1 as a therapeutic target for prostate cancer. *Mol Cancer Ther* 2014; **13**: 2361–2371.

52 Johnson IR, Parkinson-Lawrence EJ, Butler LM, Brooks DA. Prostate cell lines as models for biomarker discovery: performance of current markers and the search for new biomarkers. *Prostate* 2014; **74**: 547–560.

53 Berthon P, Cussenot O, Hopwood L, Leduc A, Maitland N. Functional expression of sv40 in normal human prostatic epithelial and fibroblastic cells - differentiation pattern of nontumorigenic cell-lines. *Int J Oncol* 1995; **6**: 333–343.

54 Fritz V, Benfodda Z, Henriquet C, Hure S, Cristol JP, Michel F et al. Metabolic intervention on lipid synthesis converging pathways abrogates prostate cancer growth. *Oncogene* 2013; **32**: 5101–5110.

55 Giordano A, Calvani M, Petillo O, Grippo P, Tuccillo F, Melone MA et al. tBid induces alterations of mitochondrial fatty acid oxidation flux by malonyl-CoA-independent inhibition of carnitine palmitoyltransferase-1. *Cell Death Differ* 2005; **12**: 603–613.

56 Priore P, Giudetti AM, Natali F, Gnoni GV, Geelen MJ. Metabolism and short-term metabolic effects of conjugated linoleic acids in rat hepatocytes. *Biochim Biophys Acta* 2007; **1771**: 1299–1307.

57 Peluso G, Petillo O, Margarucci S, Mingrone G, Greco AV, Indiveri C et al. Decreased mitochondrial carnitine translocase in skeletal muscles impairs utilization of fatty acids in insulin-resistant patients. *Front Biosci* 2002; **7**: a109–a116.

58 IJlst L, van Roermund CW, Iacobazzi V, Oosthein W, Ruiter JP, Williams JC et al. Functional analysis of mutant human carnitine acylcarnitine translocases in yeast. *Biochem Biophys Res Commun* 2001; **280**: 700–706.

59 Muoio DM, Noland RC, Kovalik JP, Seiler SE, Davies MN, DeBalsi KL et al. Muscle-specific deletion of carnitine acetyltransferase compromises glucose tolerance and metabolic flexibility. *Cell Metab* 2012; **15**: 764–777.

60 Brass EP, Hoppel CL. Relationship between acid-soluble carnitine and coenzyme A pools in vivo. *Biochem J* 1980; **190**: 495–504.

61 Kim JY, Hickner RC, Cortright RL, Dohm GL, Houmard JA. Lipid oxidation is reduced in obese human skeletal muscle. *Am J Physiol Endocrinol Metab* 2000; **279**: E1039–E1044.

62 Shahabi A, Lewinger JP, Ren J, April C, Sherrod AE, Hacia JG et al. Novel gene expression signature predictive of clinical recurrence after radical prostatectomy in early stage prostate cancer patients. *Prostate* 2016; **76**: 1239–1256.

Supplementary Information accompanies this paper on the Oncogene website (http://www.nature.com/onc)